

Journal of Materials Chemistry C

Accepted Manuscript



This is an *Accepted Manuscript*, which has been through the Royal Society of Chemistry peer review process and has been accepted for publication.

Accepted Manuscripts are published online shortly after acceptance, before technical editing, formatting and proof reading. Using this free service, authors can make their results available to the community, in citable form, before we publish the edited article. We will replace this *Accepted Manuscript* with the edited and formatted *Advance Article* as soon as it is available.

You can find more information about *Accepted Manuscripts* in the [Information for Authors](#).

Please note that technical editing may introduce minor changes to the text and/or graphics, which may alter content. The journal's standard [Terms & Conditions](#) and the [Ethical guidelines](#) still apply. In no event shall the Royal Society of Chemistry be held responsible for any errors or omissions in this *Accepted Manuscript* or any consequences arising from the use of any information it contains.

ARTICLE

Naphthalenediimide-based donor-acceptor copolymer prepared by chain-growth catalyst-transfer polycondensation: evaluation of electron-transporting properties and application in printed polymer transistors.

Cite this: DOI: 10.1039/x0xx00000x

Received 00th February 2014,
Accepted 00th May 2014

DOI: 10.1039/x0xx00000x

www.rsc.org/

G. C. Schmidt,^{a*} D. Höft,^a K. Haase,^a A. C. Hübler^a, E. Karpov,^b R. Tkachov,^b M. Stamm,^{b,c} A. Kiriy,^{b*} F. Haidu,^d D. R. T. Zahn,^d H. Yan,^e and A. Facchetti^f

The semiconducting properties of a bithiophene-naphthalene diimide copolymer (PNDIT2) prepared by Ni-catalyzed chain-growth polycondensation (P1) and commercially available N2200 synthesized by Pd-catalyzed step-growth polycondensation were compared. Both polymers show similar electron mobility of $\sim 0.2 \text{ cm}^2 \text{ V}^{-1} \text{ s}^{-1}$, as measured in top-gate OFETs with Au source/drain electrodes. It is noteworthy that the new synthesis has several technological advantages compared to traditional Stille polycondensation, as it proceeds rapidly at room temperature and does not involve toxic tin-based monomers. Furthermore, a step forward to fully printed polymeric devices was achieved. To this end, transistors with PEDOT:PSS source/drain electrodes were fabricated on plastic foils by means of mass printing technologies in a roll-to-roll printing press. Surface treatment of the printed electrodes with PEIE, which reduces the work function of PEDOT:PSS, was essential to lower the threshold voltage and achieve high electron mobility. Fully polymeric P1 and N2200-based OFETs achieved average linear and saturation FET mobilities of $>0.08 \text{ cm}^2 \text{ V}^{-1} \text{ s}^{-1}$. Hence, the performance of n-type, plastic OFET devices prepared in ambient laboratory conditions approaches those achieved by more sophisticated and expensive technologies, utilizing gold electrodes and time/energy consuming thermal annealing and lithographic steps.

Introduction

Organic thin-film transistors (OTFTs) based on semiconducting polymers are a potentially low-cost technology. Furthermore, they are an alternative to amorphous silicon transistors for applications in large-area OTFT-based arrays, for example, backplane/driver circuits for active matrix displays, where high transistor density and switching speeds are not necessary.¹ Advantages of OTFTs originate from the potential lower manufacturing costs and reduced capital investments thanks to device fabrication using common solution-based deposition and patterning techniques such as different (mass) printing technologies like inkjet,² gravure, flexo and offset printing.³ Furthermore, circuits based on conjugated polymers are compatible with plastic substrates so that compact, lightweight, structurally robust and flexible electronic devices can be fabricated.^{4,5}

n-Type (or electron-conducting) polymers are essential components in organic devices, such as ambipolar and n-

channel field-effect transistors or organic photovoltaics.⁶ Rylene diimide alternating main chain copolymers, such as those based on naphthalene diimides, are currently evolving as an intriguing class of electron-conducting materials.⁷ For example, a bithiophene-naphthalene diimide copolymer (PNDIT2, also known as P(NDI2OD-T2) and commercially available as Activink N2200) was reported to yield high electron mobilities under ambient conditions.⁸ Furthermore, PNDIT2, and its analogous, were shown to be promising electron acceptors for all-polymer solar cells.⁹ Semiconducting conjugated polymers, including PNDIT2, are generally synthesized by step-growth polymerizations, most often by Pd-catalyzed Stille polycondensation.⁷ Conjugated polymers synthesized in such a way frequently suffer from a low degree of control over molecular weight (MW). This often results in batch-to-batch variations and altered semiconducting properties, which is undesirable for optoelectronic applications. Another important drawback of step-growth polycondensations is that they are relatively slow processes so that synthesis of

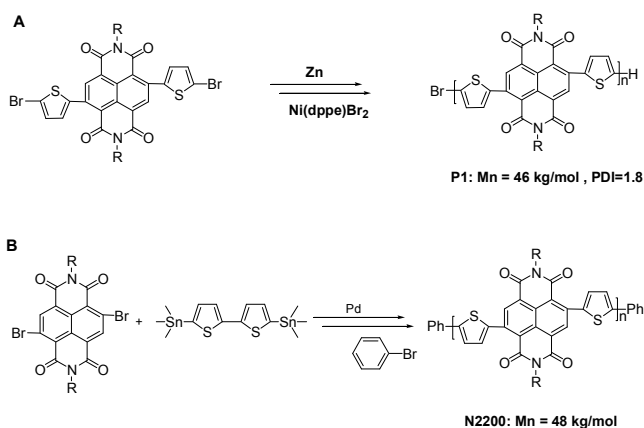
high enough MW polymers usually requires long reaction times and high reaction temperatures.¹⁰ The formation of toxic tin-based by-products is another important concern of the Stille polycondensation.¹¹

Recently, we introduced a novel nickel-catalyzed chain-growth polymerization of an anion-radical monomer that allows preparation of PNDIT2 with controlled MW and relatively low polydispersity index, PDI (Scheme 1).¹² Additional advantage of the developed polymerization is that it proceeds relatively fast (within a couple of hours) and does not use toxic tin-based monomers. To this regard, the newly-developed synthetic methodology is a promising technology for potential commercial applications. However, the semiconducting properties of PNDIT2 prepared by means of the new method were not tested in OFETs. The present work compares the semiconducting performance of PNDIT2 obtained by chain-growth tin-free polymerization and commercially available PNDIT2 prepared by Pd-catalyzed step-growth Stille polycondensation (here indicated as N2200). Furthermore, we were particularly interested in evaluating their semiconducting properties in fully-organic, printed OFET devices. Our data demonstrate the first report enabling high-mobility n-type FETs using printed PEDOT:PSS electrodes.

Experimental

Materials. In this work, PNDIT2 with $M_n = 46$ kg mol⁻¹ and PDI=1.8 (further named as P1) was synthesized by the previously reported chain-growth polycondensation method (Scheme 1A).¹¹ Commercially available N2200 with $M_w = 48$ kg mol⁻¹ and PDI=4.7, prepared by step-growth Stille polycondensation⁸ (Scheme 1B) was also used in this study. A comparison of NMR and absorption spectra of P1 and N2200 does not reveal any distinct differences in their structures.

Scheme 1. Chain-growth (A) and step-growth (B) synthesis of PNDIT2.



Preparation of TFTs with gold electrodes. The top-gate, bottom-contact OTFT devices (Fig. 1a) were fabricated on glass substrates (Precision Glass & Optics, Eagle 2000). The gold source and drain electrodes (~ 35 nm) were deposited by thermal evaporation using a shadow mask ($L = 50$ μm , $W = 500$ μm). The semiconductor films were spin-coated in a N_2 glovebox from polymer solutions having a concentration of 8 mg/ml in ortho-dichlorobenzene. Then, CYTOP (Asahi Glass CTL-809M) diluted with CT Solv-180 at the ratio of 3:1 was

spun coated at 1500 RPM for 60 s as the dielectric layer. The dielectric film was then baked at 110 $^\circ\text{C}$ on a hotplate for 10 min before the deposition of a ~ 35 nm gold thin film as the gate electrode. The measured capacitance of the CYTOP dielectric layer was 3.5 nF cm⁻². The completed devices were tested in ambient.

Preparation of fully plastic devices with mass printed PEDOT:PSS source/drain electrodes. PEDOT:PSS source/drain electrodes were fabricated on highly flexible and low-cost plastic foils (PET, 100 μm thick) by means of mass printing technologies with a roll-to-roll (R2R) printing press with a printing speed of 0.3 m s⁻¹ (Fig. 1). Details of this so called “Cyflex” technology, which is a combination of flexography and gravure printing, were described elsewhere.^{13,14} Using PEDOT:PSS as material for the electrodes is a promising approach³ because of the very good compatibility to R2R processes and the production of low cost, environmentally friendly electronics (Figure 1b-d).

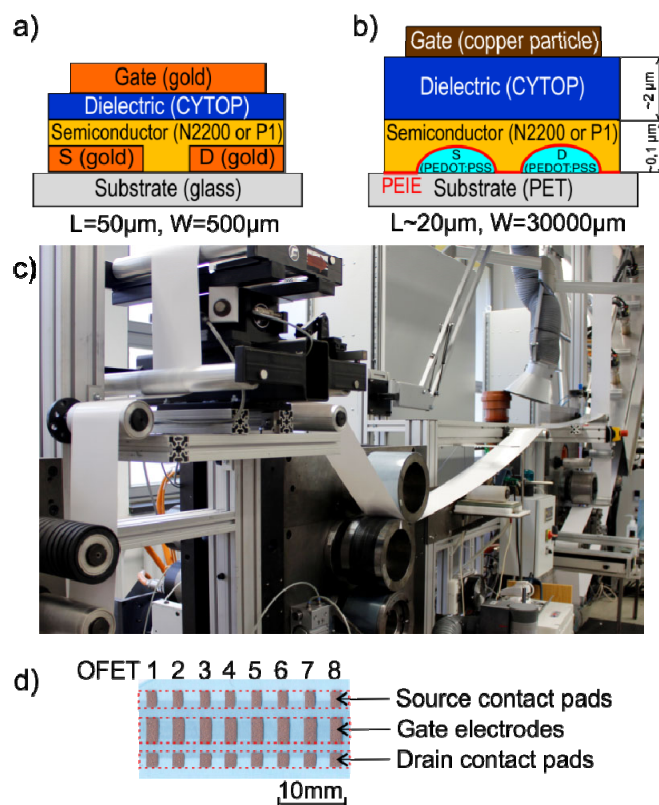


Figure 1. Schematics of OFETs fabricated with a) thermally evaporated gold electrodes and b) printed polymeric/metal electrodes, c) R2R printing press with two printing units for the fabrication of source/drain electrodes, d) Photograph of a printed sample with 8 polymeric OFETs. Source/drain contact pads connecting 10 channels, leading to a channel width of 30,000 μm .

PEDOT:PSS is a well-known conductor exhibiting good hole injection properties. Thus, when using PEDOT:PSS as an electron injecting material there is a need for surface modification to fine-tune the work function. Therefore, the PEDOT:PSS electrodes were optionally treated by ethoxylated poly(ethyleneimine) (PEIE) to reduce the work function of the electrodes.¹⁵ This process step is quite important for good

electron injection, because of the high work function of printed PEDOT:PSS source/drain electrodes which was measured to be 5.4–5.7 eV.¹⁴ PEIE, 80% ethoxylated, dissolved in water at a concentration of 35–40 wt.% was received from Sigma and further diluted with butyl glycol to a final concentration of 0.4 wt.%. This solution was spincoated on top of the PEDOT:PSS source/drain electrodes, next the film was dried at 110 °C for 5 min. Afterwards, either P1 or N2200 were deposited from a 1 wt.% solution in xylene by means of spincoating, followed by a drying step at 110 °C for 10 min. As dielectric CYTOP CTL-809M was used as received and applied via spincoating, resulting in a layer thickness of ~2 μm after drying at 110 °C for 10 min. This leads to a maximum specific gate capacitance in accumulation regime of 1.1–1.2 nF cm⁻². The higher thickness of the dielectric was chosen to prevent high gate leakage current for the printed devices. Finally, the gate electrodes were flexo-printed at a laboratory printing press (Flexiproof 100, RK Print) with a copper micro-particle ink received from Eckart. To achieve sufficient wetting of the ink printed onto the hydrophobic CYTOP layer, the surface tension of the formulation was reduced by adding perfluoro surfactants. Additionally, the printing settings velocity and pressure between the rollers were optimized to get homogenous and well structured gate electrodes. Due to the relatively low pressure between the printing rollers and the flexible substrate, flexography prevents the sensitive organic layers from very high mechanical stress while printing the gate. The channel length and the channel width of these OFETs were 20 μm and 30,000 μm, respectively. All process steps and measurements were executed under ambient laboratory conditions in air.

Results and discussion

Mobility of devices with gold electrodes. We first compared the semiconducting properties of P1 and N2200 by fabricating conventional TFTs on glass substrates and using Au source/drains electrodes, CYTOP as the gate dielectric, and silver as top gate electrode. The top-gate device architecture was selected because it is the best architecture for this type of polymers.⁸ Polymer semiconductor and gate dielectric layers were deposited in ambient conditions. The N2200 control sample afforded electron mobilities of 0.1–0.29 cm² V⁻¹ s⁻¹ and on/off ratios ~ 10⁶, which are in performance very close to the literature values. P1 prepared by the chain-growth polycondensation showed very similar electron mobilities of 0.1–0.2 cm² V⁻¹ s⁻¹ and on/off ratios ~ 10⁶. Typical transfer characteristics for these transistors are reported in Figure 2. The most important difference between the polymer prepared in this work and the commercial available N2200 is that P1 exhibited more pronounced ambipolar behavior, with hole mobilities ~ 10⁻² cm² V⁻¹ s⁻¹. N2200 exhibited about two orders of magnitude lower hole mobilities. Although the origin of the performance variation in these structurally similar polymers is unclear at the moment, different polymer end-group structure (H/Br in P1 versus Ph-termination in N2200) and residual metal content may play a role.⁸ As such, the most important conclusion is that the reaction conditions of the newly developed polymerization do not affect substantially the electron transporting properties of the resulting polymers and electronic grade semiconducting polymers can be prepared, obviously upon further synthetic optimization, with this method.

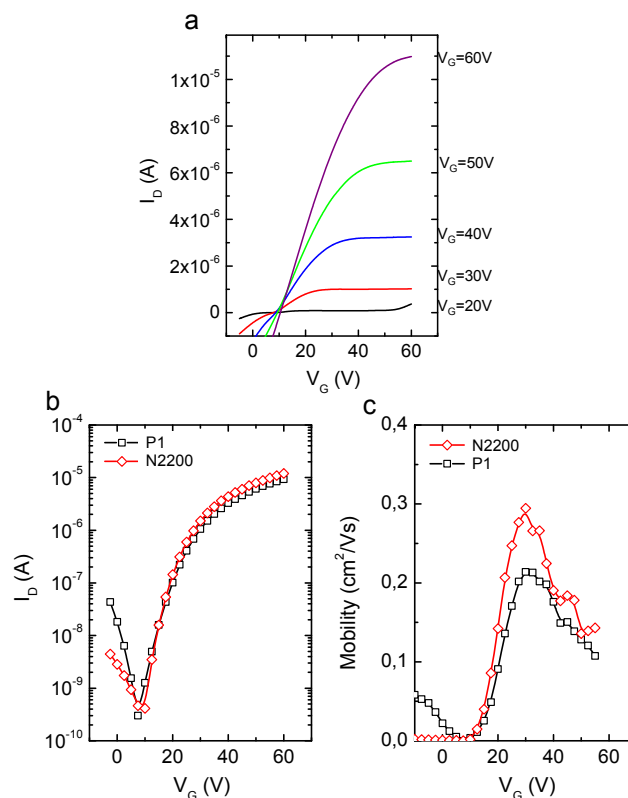


Figure 2. Output characteristics of the representative OFET made with P1 fabricated on glass by using Au electrodes and CYTOP as dielectric (a); comparison of transfer curves of OFETs obtained with P1 and N2200 (b); mobility evolution curves for P1 and N2200 (c). Note, in these devices the semiconductor and the gate contact were not patterned.

Fully plastic devices fabricated with mass printed PEDOT:PSS source/drain electrodes. Commercially available PEDOT:PSS was used in this work for the fabrication of the source/drain electrodes. PEDOT:PSS is a good hole injection material because its work function of about -5.4 eV fits well to HOMO energy levels of many organic semiconductors (Figure 3).

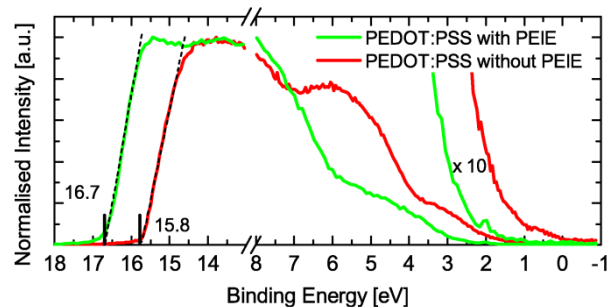


Figure 3. UPS spectra of printed PEDOT:PSS layers with and without PEIE layer on top. From the secondary electron cutoff a work function of -4.5 eV and -5.4 eV can be calculated.

However, it is likely the work function of PEDOT:PSS is too high for efficient injection of electrons into the LUMO of

organic n-type semiconductors. It was recently demonstrated that the work function of conductors, including metals, transparent conductive metal oxides and conducting polymers can be significantly reduced by adsorption of surface modifiers containing aliphatic amine groups, such as ethoxylated poly(ethyleneimine) (PEIE).¹⁵ Thus, to rationalize the performance of our devices (*vide infra*), UPS measurements of printed PEDOT:PSS layers with and without PEIE coating were carried out and the results are shown in Fig. 3. These data indicate a considerable decrease of the PEDOT:PSS work function upon PEIE treatment from (-5.4 ± 0.1) eV to (-4.5 ± 0.1) eV.

Therefore, in this work, the OFET performances of n-channel polymers such as P1 and N2200 were evaluated for the first time using printed PEDOT:PSS electrodes with and without PEIE treatment. These devices have been fabricated by spin-coating the semiconductor (P1 or N2200) and the dielectric (CYTOP) on top of the source/drain electrodes. Finally, the gate electrodes (copper-particle ink) were printed by flexography. Typical output and transfer curves of these OFETs are given in Figure 4. It becomes obvious that the PEIE treatment strongly improves the electrical contact between the polymeric electrodes and the semiconductor. The devices without PEIE injection layer (Figure 4a and c) required a very high source/drain voltage V_{ds} to overcome the high contact resistance resulting from the mismatch between PEDOT:PSS (-5.4 eV) and the LUMO level of PNDIT2 (-4.0 eV). Thus, the threshold voltage of the devices without PEIE treatment was found to be $+20.0$ and $+22.8$ V for N2200 and P1, respectively.

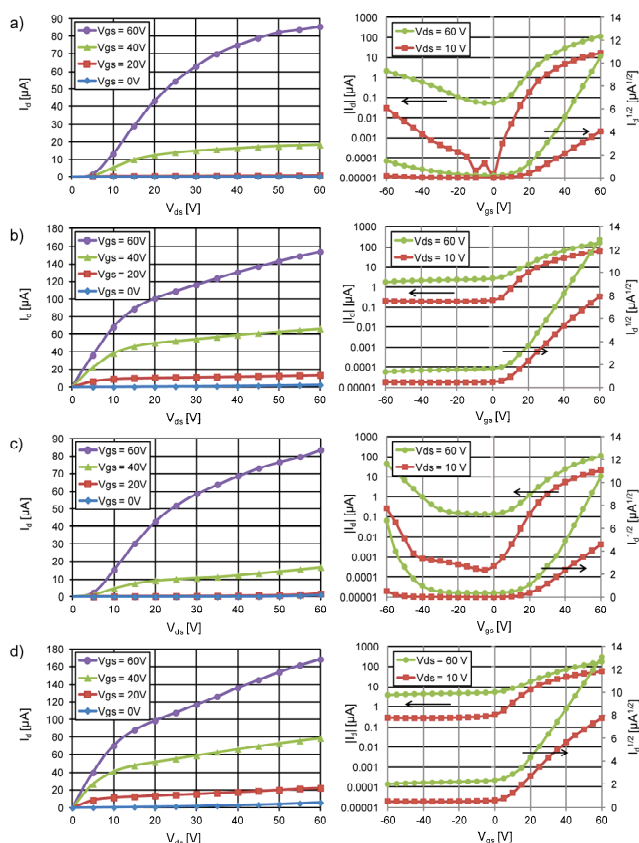


Figure 4. Output (left) and transfer (right) curves of OFETs made with a) N2200 without PEIE, b) N2200 with PEIE treatment, c) P1 without PEIE, and d) P1 with PEIE treatment.

In contrast, OFETs fabricated with PEIE show a typical linear increase of the drain current I_d for low V_{ds} as the result of the decreased PEDOT:PSS work function and the threshold voltage of these devices decreases to $+9.9$ and $+10.6$ V, respectively. Besides other important parameters, a low threshold voltage is essential to decrease the supply voltage for printed circuits based on fully polymeric/organic FETs. Thus, our results strongly indicate the possibility to print fully polymeric n-type OFETs.

Fully polymeric N2200-based OFETs with the PEIE treatment achieved mean linear and saturation electron mobilities of 0.08 and $0.05 \text{ cm}^2 \text{ V}^{-1} \text{ s}^{-1}$, respectively (Table 1). Very similar results could be obtained when using P1 instead of N2200, in which both mobilities in the linear and saturation regimes were found to be $0.08 \text{ cm}^2 \text{ V}^{-1} \text{ s}^{-1}$ as well. Take notice that these improved mobility values are not significantly influenced by different gate leakage current levels ($I_{g,max} < 10 \text{ nA}$). These mobility values are somewhat lower than those achieved for OFETs based on gold electrodes. However, our all-polymeric devices, which include a flexible substrate, were prepared under ambient laboratory conditions in air and without thermal evaporation and lithographic processing steps. Interestingly, the significant ambipolar transport observed for P1-based OFETs and gold electrodes was found for devices without PEIE treatment. The ambipolar transport was suppressed by the PEIE treatment of the electrodes indicating the strong hole blocking property of PEIE.

An overview of all electrical parameters for the OFETs fabricated with PEDOT:PSS source/drain electrodes are given in Table. Clearly our results indicate that PEIE treatment greatly improves electron injection, reduces the threshold voltage and enhances the carrier mobility. However, Table 1 clearly indicates that the current on-off ratios decrease upon PEIE treatment, a result originating by the increased off-current. Since the PEIE coating is not only present on top of the electrodes but also in the channel area below the semiconductor, PEIE doping of the semiconductor leads to a higher intrinsic conductivity and thus reduced current on-off ratio. The doping effect was mentioned earlier by Zhou and co-workers.¹⁵ However, this drawback could be overcome by selective treatment of the electrical contacts by printing PEIE instead of spin-coating the formulation. Furthermore, fine patterning of the semiconductor, as required for circuit application, will further enhance the on-off ratio.

Table 1. Comparison of the most important electrical parameters of OFETs made on the basis of PEDOT:PSS source/drain electrodes with the semiconductor N2200 or P1.

Semi-conductor	PEIE	$\mu_{e,lin}$ ($\text{cm}^2 \text{ V}^{-1} \text{ s}^{-1}$)	$\mu_{e,sat}$ ($\text{cm}^2 \text{ V}^{-1} \text{ s}^{-1}$)	V_{th} (V)	I_{ON}/I_{OFF}
N2200 (6 OFETs)	no	0.035 ± 0.009	0.077 ± 0.023	20.0 ± 0.9	$2,003 \pm 342$
N2200 (7 OFETs)	yes	0.080 ± 0.028	0.052 ± 0.023	9.9 ± 0.8	61 ± 12
P1 (7 OFETs)	no	0.037 ± 0.008	0.075 ± 0.019	22.8 ± 1.2	$1,250 \pm 1,110$
P1 (7 OFETs)	yes	0.086 ± 0.014	0.080 ± 0.030	10.6 ± 1.4	30 ± 15

Conclusions

In the present work, we have compared the semiconducting properties of PNDIT2 prepared by Ni-catalyzed chain-growth polycondensation (P1) and the commercially available N2200 synthesized by Pd-catalyzed step-growth polycondensation. Despite of different synthetic methodologies P1 and N2200 exhibit similar electron mobilities of $\sim 0.2 \text{ cm}^2 \text{ V}^{-1} \text{ s}^{-1}$ for top-gate OFET devices having gold source/drain electrodes. The first printed n-channel polymeric devices were also fabricated by printing PEDOT:PSS source/drain electrodes on highly flexible plastic foils. Treatment of the plastic electrodes with PEIE, which significantly reduces the work function of PEDOT:PSS, was found to be essential for lowering of the threshold voltage and achieving high electron mobilities ($0.08 \text{ cm}^2 \text{ V}^{-1} \text{ s}^{-1}$) for both P1- and N2200-based devices. Hence, the performance of our flexible devices fabricated in ambient laboratory conditions approaches the performance of OFETs fabricated by means of much more sophisticated and expensive processes, utilizing gold electrodes and time/energy consuming thermal annealing and lithographic steps. Finally, it is noteworthy to point out that the new synthesis has several technological advantages compared to traditional Stille polycondensation, as it proceeds fast at room temperature and does not involve toxic tin-based monomers. As such, this is a substantial step toward commercialization of fully plastic transistors.

Acknowledgements

AK, MS and GS gratefully acknowledge support from DFG within the German Excellence Initiative via the Cluster of Excellence EXC 1056 "Center for Advancing Electronics Dresden" (cfAED). Furthermore AK acknowledges support from DFG (SPP 1355 "Elementary Processes of Organic Photovoltaics", grant KI-1094/4) and GS acknowledges financial support from the European Commission for the project no. FP7-287568 (integrated project FLEXIBILITY, www.flexibility-fp7.eu). AF thanks KAU for partial support.

Notes and references

^aInstitute for Print and Media Technology, Chemnitz University of Technology, 09107 Chemnitz, Germany

^bLeibniz-Institut für Polymerforschung Dresden e.V. Hohe Straße 6, 01069 Dresden, Germany

^cTechnische Universität Dresden, Center for Advancing Electronics Dresden (cfaed), 01062, Dresden, Germany.

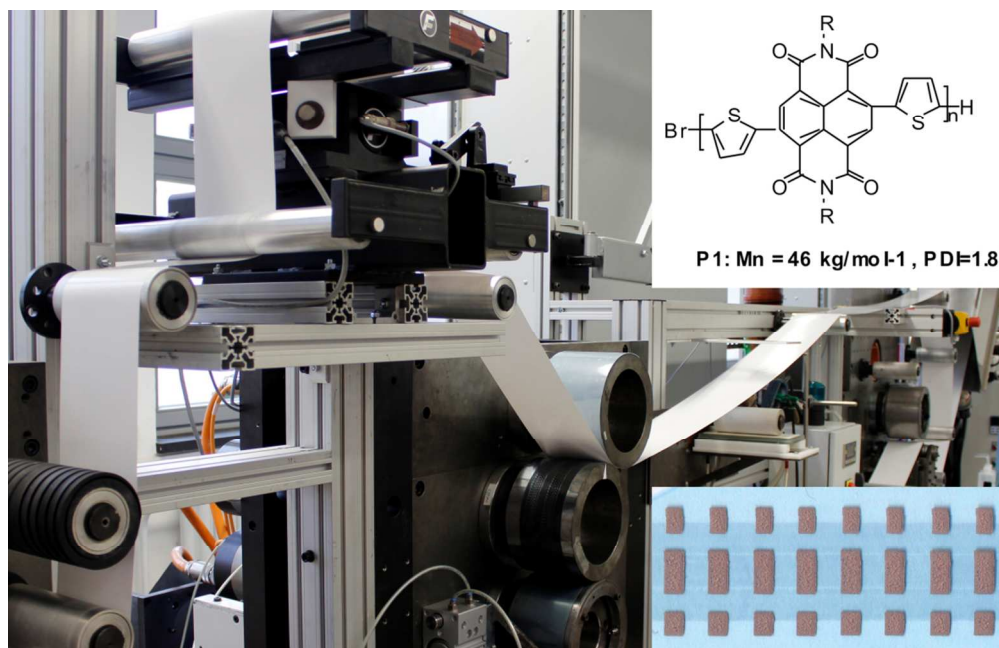
^dSemiconductor Physics, Chemnitz University of Technology, 09107 Chemnitz, Germany

^eDepartment of chemistry, The Hong Kong University of Science and Technology Clear Water Bay, Kowloon, Hong Kong

^fPolyera Corporation, 8045 Lamont Avenue, Skokie, Illinois 60077, USA and King Abdulaziz University, Jeddah 21589, Saudi Arabia.

- 1 A. Facchetti. *Chem. Mater.*, 2011, **23**, 733. H. Sirringhaus, *Adv. Mater.*, 2005, **17**, 2411. J. Smith, W. Zhang, R. Sougrat, K. Zhao, R. Li, D. Cha, A. Amassian, M. Heeney, I. McCulloch and T. D. Anthopoulos, *Adv. Mater.*, 2012, **24**, 2441. H. Chen, Y. Guo, G. Yu, Y. Zhao, J. Zhang, D. Gao, H. Liu and Y. Liu, *Adv. Mater.*, 2012, **24**, 4618.
- 2 A. Teichler, J. Perelaer and U. S. Schubert. *J. Mater. Chem. C*, 2013, **1**, 1910. S. Y. Cho, J. M. Ko, J. Lim, J. Y. Lee and C. Lee. *J. Mater. Chem. C*, 2013, **1**, 914–923
- 3 D. Zielke, A. C. Hübler, U. Hahn, N. Brandt, M. Bartzsch, U. Fügmann, T. Fischer, J. Veres and S. Ogier, *Appl. Phys. Lett.* 2005, **87**, 12, 123508-123510. A. C. Hübler, F. Dötz, H. Kempa, H. E. Katz, M. Bartzsch, N. Brandt, I. Hennig, U. Fügmann, S. Vaidyanathan, J. Granstrom, S. Liu, T. Zillger, G. Schmidt, K. Preissler, E. Reichmanis, T. Weber, P. Eckerle, F. Richter, T. Fischer and U. Hahn, *Org. Electr.*, 2007, **8**, 5, 480-486. H. Kempa, M.

- Hamsch, K. Reuter, M. Stanel, G. C. Schmidt, B. Meier and A. C. Hübler, *IEEE Trans. on Electr. Dev.*, 2011, **58**, 8, 2765–2769.
- 4 G. H. Gelinck, H. E. A. Huitema, E. V. Veenendaal, E. Cantatore, L. Schrijnemakers, J. B. P. H. V. D. Putten, T. C. T. Geuns, M. Beenhakkers, J. B. Giesbers, B.-H. Huisman, E. J. Meijer, E. M. Benito, F. J. Touwslager, A. W. Marsman, B. J. E. V. Rens and D. M. de Leeuw, *Nat. Mater.*, 2004, **3**, 106. H. E. Katz, *Chem. Mater.*, 2004, **16**, 4748. Y.-Y. Noh, N. Zhao, M. Caironi and H. Sirringhaus, *Nat. Nanotechnol.*, 2007, **2**, 784. K.-J. Baeg, D. Khim, D.-Y. Kim, S.-W. Jung, J. B. Koo, I.-K. You, H. Yan, A. Facchetti and Y.-Y. Noh, *J. Polym. Sci., Part B: Polym. Phys.*, 2011, **49**, 62. D. Khim, K.-J. Baeg, B.-K. Yu, S.-J. Kang, M. Kang, Z. Chen, A. Facchetti, D.-Y. Kim and Y.-Y. Noh. *J. Mater. Chem. C*, 2013, **1**, 1500.
- 5 T. Sekitani, T. Someya, *Adv. Mater.* **2010**, **22**, 2228-2246.
- 6 X. Zhan, Z. Tan, B. An, Z. Domercq, X. Zhang, S. Barlow, Y. Li, D. Zhu, B. Kippelen and S. R. Marder, *J. Am. Chem. Soc.*, 2007, **129**, 7246. Z. Chen, Y. Zheng, H. Yan and A. Facchetti, *J. Am. Chem. Soc.*, 2009, **131**, 8. X. Zhao, L. Ma, L. Zhang, Y. Wen, J. Chen, Z. Shuai, Y. Liu, and X. Zhan, *Macromolecules*, 2013, **46**, 2152-2158. X. Zhao and X. Zhan, *Chem. Soc. Rev.*, 2011, **40**, 3728–3743. J. E. Anthony, A. Facchetti, M. Heeney, S. R. Marder, and X. Zhan, *Adv. Mater.*, 2010, **22**, 3876-3892. X. Zhan, A. Facchetti, S. Barlow, T. J. Marks, M. A. Ratner, M. R. Wasielewski, and S. R. Marder, *Adv. Mater.*, 2011, **23**, 268-284.
- 7 E. Kozma and M. Catellani, *Dyes and Pigments*, 2013, **98**, 160. E. Zhou, J. Cong, Q. Wei, K. Tajima, C. Yang and K. Hashimoto, *Angew. Chem.*, 2011, **50**, 2799. A. Facchetti, *Materials Today*, 2013, **16**, 123. R. Steyrleuthner, M. Schubert, F. Jaiser, J. C. Blakesley, Z. Chen, A. Facchetti, D. Neher, *Adv. Mater.*, 2010, **22**, 2799. M. M. Durbán, P. D. Kazarinoff, C. K. Luscombe, *Macromolecules*, 2010, **43**, 6348.
- 8 H. Yan, Z. Chen, Y. Zheng, C. Newman, J. R. Quinn, F. Dötz, M. Kastler, A. Facchetti, *Nature* 2009, **457**, 679.
- 9 A. Facchetti, *Materials Today* **2013**, **16**, 123. R. Steyrleuthner, M. Schubert, I. A. Howard, B. Klaumunzer, K. Schilling, Z. Chen, P. Saalfrank, F. Laquai, A. Facchetti, D. Neher, *J. Am. Chem. Soc.* 2012, **134**, 18303. M. Schubert, D. Dolfen, J. Frisch, S. Roland, R. Steyrleuthner, B. Stiller, Z. Chen, U. Scherf, N. Koch, A. Facchetti and D. Neher, *Adv. Energy Mater.*, 2012, **2**, 369–380.
- 10 J. Li, Y. Zhao, H. S. Tan, Y. L. Guo, C. A. Di, G. Yu, Y. Q. Liu, M. Lin, S. H. Lim, Y. Zhou, H. Su, B. S. Ong. *Sci. Rep.*, 2012, **2**, 754. H. N. Tsao, D. M. Cho, I. Park, M. R. Hansen, A. Mavrinskiy, D. Y. Yoon, R. Graf, W. Pisula, H. W. Spiess, K. Müllen, *J. Am. Chem. Soc.* 2011, **133**, 2605.
- 11 B. Carsten, F. He, H. J. Son, T. Xu, L. Yu, *Chem. Rev.*, 2011, **111**, 1493.
- 12 V. Senkovskyy, R. Tkachov, H. Komber, M. Sommer, M. Heuken, B. Voit, W. T. S. Huck, V. Kataev, A. Petr, A. Kiriy, *J. Am. Chem. Soc.* 2011, **131**, 19966. V. Senkovskyy, R. Tkachov, H. Komber, A. John, J.-U. Sommer, A. Kiriy, *Macromolecules* 2012, **5**, 7770.
- 13 G. C. Schmidt, M. Bellmann, B. Meier, M. Hamsch, K. Reuter, H. Kempa, and A.C. Hübler, *Org. Electr.*, 2010, **11**, 1683.
- 14 G. C. Schmidt, D. Höft, M. Bhuie, K. Haase, M. Bellmann, F. Haidu, D. Lehmann, D. R. T. Zahn, and A. C. Hübler, *Appl. Phys. Lett.*, 2013, **103**, 113302-1-4.
- 15 Y. Zhou, C. Fuentes-Hernandez, J. Shim, J. Meyer, A. J. Giordano, H. Li, P. Winget, T. Papadopoulos, H. Cheun, J. Kim, M. Fenoll, A. Dindar, W. Haske, E. Najafabadi, T. M. Khan, H. Sojoudi, S. Barlow, S. Graham, J.-L. Brédas, S. R. Marder, A. Kahn and B. Kippelen, *Science*, 2012, **336**, 327



99x64mm (300 x 300 DPI)